10.1515/astro-2017-0128

Baltic Astronomy, vol. 25, 261–266, 2016

ESTIMATING THE VERTICAL DISK SCALE HEIGHT USING YOUNG GALACTIC OBJECTS

V. V. Bobylev and A. T. Bajkova

Central (Pulkovo) Astronomical Observatory of RAS, 65/1 Pulkovskoye Ch., St. Petersburg, Russia; bob-v-vzz@rambler.ru

Received: 2016 September 27; accepted: 2016 October 17

Abstract. We compiled published data on young Galactic objects such as masers with VLBI-measured trigonometric parallaxes, OB associations, H II regions and Cepheids. We have recently established that the vertical disk scale height is strongly influenced by objects of the Local arm. In this study we use samples that do not contain objects in this arm and derive the following vertical disk scale heights in terms of the self-gravitating isothermal disk model for the density distribution: $h = 46 \pm 5$ pc for 69 masers with trigonometric parallaxes, $h = 36 \pm 3$ pc for 59 OB associations, $h = 35.6 \pm 2.7$ pc for 147 H II regions, $h = 52.1 \pm 1.9$ pc for 195 young Cepheids, and $h = 72.0 \pm 2.3$ pc for 192 old Cepheids.

Key words: ISM: structure – Galaxy (Milky Way): kinematics and dynamics

1. INTRODUCTION

The Galactic thin disk attracts the attention of many authors who use the data on young O- and B-type stars, open clusters, Cepheids, infrared sources, molecular clouds, and other young objects to study its properties. Of particular importance are such parameters as the offset of the symmetry plane relative to the Sun, $z_\odot$, and the vertical disk scale height h.

In our earlier study (Bobylev & Bajkova 2016a) we demonstrated that the z distribution of Galactic masers with measured trigonometric parallaxes is asymmetric. We suggested that this is because the sample is dominated by the masers observed mainly from the Earth's northern hemisphere. However, other factors may also be responsible for this peculiarity, which should be studied using a large statistical material. In particular, it is of interest to check the influence of the Local arm. As we showed previously (Bobylev & Bajkova 2014), the symmetry plane of the Local arm is tilted by about 6° to the Galactic plane. The effect on the results can be quite significant given that about 40 of the 130 masers belong to the Local arm.

Bobylev & Bajkova (2016b) used an approach based on the exclusion of Local-arm objects to analyze samples of Galactic objects with kinematically determined distances. In this paper, we apply this approach to samples consisting of objects with distances with higher accuracy, from 10% (trigonometric parallaxes) to 15%–25% ("period-luminosity" or spectrophotometric distances).

2. METHOD

We use heliocentric Cartesian coordinate systems xyz where the x, y, and z axes point toward the Galactic center, in the direction of the Galactic rotation, and toward the north Galactic pole, respectively.

In the case of exponential density distribution, the observed distribution of objects along the z coordinate axis is described by the formula

$$N(z) = N_1 \exp\left(-\frac{|z - z_\odot|}{h_1}\right). \tag{1}$$

In the self-gravitating isothermal disk model the observed distribution of objects along the z axis is described by formula

$$N(z) = N_2 \operatorname{sech}^2\left(\frac{z - z_\odot}{\sqrt{2}\, h_2}\right). \tag{2}$$

Finally, the observed distribution of objects along the z axis for the Gaussian model is described by the formula

$$N(z) = N_3 \exp\left[-\frac{1}{2}\left(\frac{z - z_\odot}{h_3}\right)^2\right]. \tag{3}$$

In (1)–(3), N_i, $i = 1, 2, 3$, are the normalization coefficients, $z_\odot$ is the offset of the symmetry plane relative to the Sun, and h_i are vertical disk scale parameters (in the case of $i = 1$, h_i is the so-called "scale height").

3. DATA

(1) We use the data on known OB associations with reliable distance estimates from Mel'nik & Dambis (2009). The distances derived by these authors were reconciled with the Cepheid scale. The catalog contains 91 OB associations and their heliocentric distances do not exceed 3.5 kpc.

(2) We use a sample of Galactic masers with measured trigonometric parallaxes. These sources, which are associated with very young stars, reside in regions of ongoing star formation. Highly accurate astrometric VLBI measurements of trigonometric parallaxes and proper motions have already been performed for more than 130 such masers by several teams in the USA, Japan, Europe, and Australia (Reid et al. 2014; Bobylev et al. 2016; Rastorguev et al. 2016). The errors of stellar parallaxes determined by this method are, on average, less than 10%. For these objects we impose a distance cut leaving only objects with heliocentric distances $r < 6$ kpc. We apply heliocentric distance cuts to all samples in order to avoid the influence of the disk warp (Bobylev 2013).

(3) We supplemented the well-known catalog of H II regions (Russeil 2003) with new photometric distance estimates for several star-forming regions, collected in Russeil et al. (2007) and Moisés et al. (2011). From this catalog we adopt only those distances that were obtained photometrically and apply the $r < 4.5$ kpc distance cut to these objects.

(4) We use the sample of Galactic classical Cepheids from Mel'nik et al. (2015). This sample contains 674 stars with the distances determined from the most recent calibrations using both optical and infrared photometric observational data. We

Table 1. The offset of the symmetry plane relative to the Sun, $z_\odot$, and the vertical disk scale height h_i, $i = 1, 2, 3$, inferred in terms of models (1), (2) and (3) from the samples with trigonometric, spectrophotometric or "period-luminosity" based distances.

$z_\odot$, pc	h_1, pc	h_2, pc	h_3, pc	Sample
-18 ± 5	51 ± 5	46 ± 5	54 ± 5	69 masers with parallaxes
-13 ± 4	46 ± 3	36 ± 3	45 ± 3	59 OB associations
-14 ± 4	46.6 ± 2.8	35.6 ± 2.7	48.4 ± 2.8	147 H II regions
-26 ± 2	64.1 ± 2.4	52.1 ± 1.9	68.2 ± 2.5	195 young Cepheids
-26 ± 2	83.1 ± 2.4	72.0 ± 2.3	85.2 ± 2.8	192 old Cepheids

have two samples of Cepheids with mean ages ≈75 Myr and ≈138 Myr and leave only only objects with $r < 4$ kpc.

We adopted the simplest Local-arm model in the form of a 6.2×1.1 kpc rectangle turned by angle -13° to the y axis and shifted from the Sun by 0.3 kpc toward the Galactic anticenter (see Figs. 1–2 in Bobylev & Bajkova 2016b). For the sample of masers with measured trigonometric parallaxes we use the partition into spiral arms according to Reid et al. (2014).

4. RESULTS AND DISCUSSION

Table 1 lists the offset of the symmetry plane relative to the Sun, $z_\odot$, and the vertical disk scale height h_i, $i = 1, 2, 3$, estimates obtained using models (1)–(3). We determined these parameters and their errors by fitting the models to the histograms and via Monte-Carlo simulations. For this purpose, we constructed the histograms with a bin size of 20 pc in z coordinate. As is evident from Table 1, h_1 and h_3 values are close to each other, and we therefore show only two curves in Figs. 1 and 2: one for model (1) and one for model (2).

The unshaded histogram in the left panel of Fig. 1 is based on the whole sample of 113 masers ($r < 6$ kpc). The shaded histogram in the left panel of Fig. 1 was constructed using 44 masers of the Local arm. As can be clearly seen from this figure, the peak of the distribution of the Local-arm masers is located at positive z. Moreover, the strong influence of Local-arm masers on the distribution of the entire sample is immediately apparent, leading us to conclude that Local arm objects have to be excluded. The right panel of Fig. 1 shows the histogram constructed using 69 masers, without objects of the Local arm.

Figure 2 shows the histograms for OB associations, H II regions, young and old Cepheids. A comparison with the results obtained from the same samples without excluding Local-arm objects (Bobylev & Bajkova 2016a) demonstrates a significant improvement for the histograms (they become closer to the Gaussian) of masers and OB associations. Previously (Bobylev & Bajkova 2016a), we found the following vertical disk scale height estimates: $h_2 = 40.2 \pm 2.1$ pc from 91 OB associations, $h_2 = 48.4 \pm 2.5$ pc from 187 H II regions, $h_2 = 60.1 \pm 1.9$ pc from 246 young Cepheids, and $h_2 = 72.5 \pm 2.3$ pc from 250 old Cepheids. The scale height h can be seen to always decrease after the exclusion of Local-arm objects.

Bobylev & Bajkova (2016b) obtained the following estimates from an analysis of objects located in the inner region of the Galaxy: $z_\odot = -5.7 \pm 0.5$ pc and $h_2 = 24.1 \pm 0.9$ pc from the sample of 639 methanol masers, $z_\odot = -7.6 \pm 0.4$ pc and $h_2 = 28.6 \pm 0.5$ pc from 878 H II regions, $z_\odot = -10.1 \pm 0.5$ pc and $h_2 = 28.2 \pm 0.6$ pc from 538 giant molecular clouds.

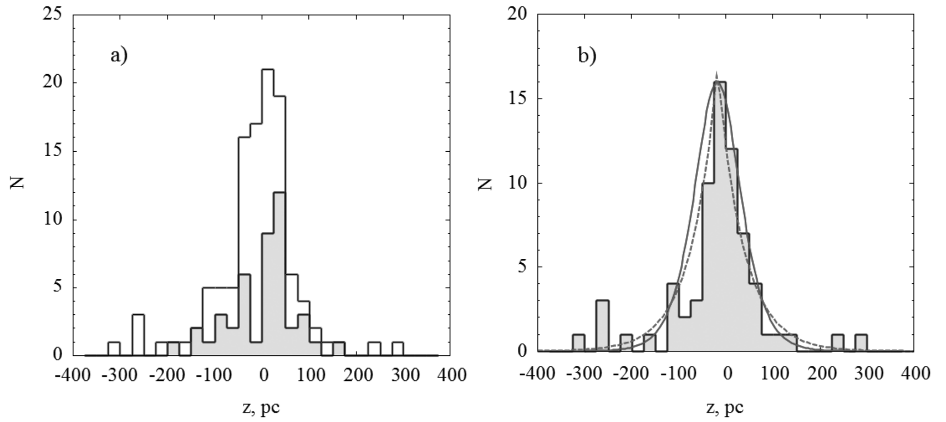

Fig. 1. Histograms of the z distribution of masers: (a) the whole sample (unshaded) and the masers belonging to the Local-arm only (shaded); (b) the sample without Local-arm masers, with the dashed and solid lines representing models (1) and (2), respectively.

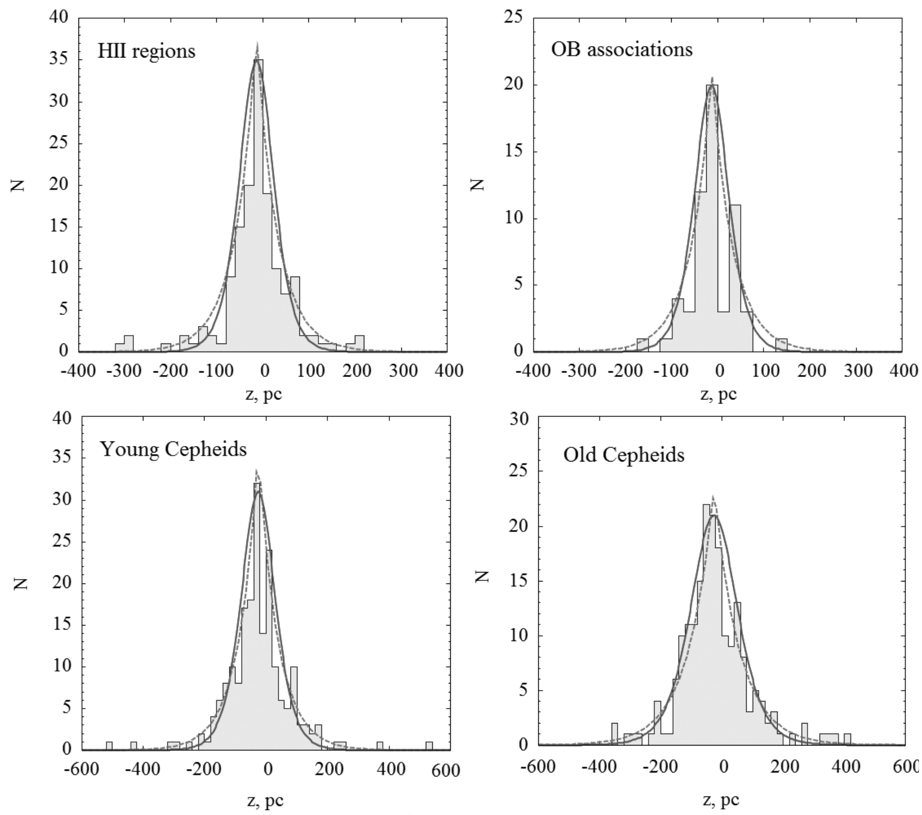

Fig. 2. Histograms of the z distributions of 59 OB associations, 147 H II regions, 195 young Cepheids and 192 old Cepheids. The dashed and solid lines in all panels represent models (1) and (2), respectively.

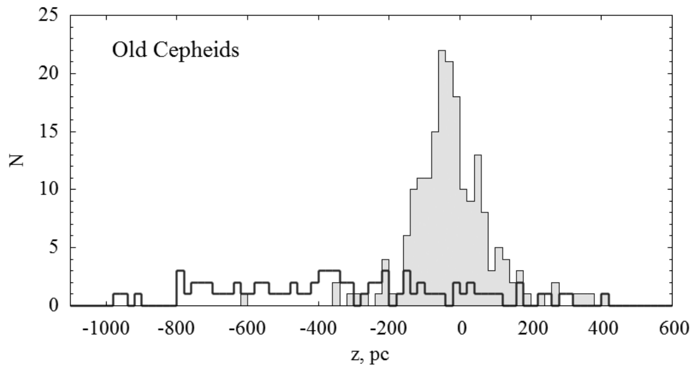

Fig. 3. Histograms of the z distribution of old Cepheids: the sample with heliocentric distance $4 < r < 10$ kpc (unshaded) and the sample with distances $r < 4$ kpc (shaded).

For a detailed review of the parameters $z_\odot$ and h obtained by different authors see Bobylev & Bajkova (2016a). Here we only note the result of the analysis of the extensive sample of giant molecular clouds (the ATLASGAL program) with kinematic distances adopted from Wienen et al. (2015). These authors found $z_\odot \sim -7 \pm 1$ pc and $h \sim 28 \pm 2$ pc.

It is interesting that the histograms of the z distributions for practically all of the samples studied show broad wings (see Figs. 1–2), with the exception of OB associations. The wings are also visible in the histogram for Wolf-Rayet stars (Fig. 2 in Bobylev & Bajkova 2016a) and methanol masers (Fig. 6 in Bobylev & Bajkova 2016b). We thus see that (i) the histogram wings are always better approximated by model (1), (ii) none of the three models can fully describe the broad wings.

A detailed study of all effects leading to the formation of broad wings of the histograms is the subject of a separate study due to the great complexity of the problem. Here we would like to mention only one of the possible causes associated with the warp of the galactic disk (Bobylev 2013). To this end, we use old Cepheids. In Fig. 3 there are two histograms constructed for two different samples. The first sample consists of 192 Cepheids, located at distances $r < 4$ kpc (also shown in Fig. 2) and the second sample includes 81 Cepheids in the distance interval $4 < r < 10$ kpc. As can be seen from Fig. 3, the distribution of distant Cepheids (second sample) is shifted considerably toward negative z and has a much greater variance compared to the distribution for the Cepheids of the first sample: it can be described, for example, in terms of model (3) with the following parameters: $z_\odot = -321$ pc and $h_3 = 241$ pc. We thus have two distributions with very different properties. Hence the broad wings of the histograms of the z-distributions may be a result of the penetration of objects with properties of the second sample into the first sample due to large measurement errors of the distances of the objects.

5. CONCLUSIONS

To study the vertical distribution of visible matter in the thin disk of the Galaxy we used several samples of young objects in the solar neighborhood located within 4.5 kpc (6 kpc for masers) from the Sun. We show that as far as our study is concerned, it is better to exclude Local-arm objects from the sample of masers with measured parallaxes.

We fitted the vertical distributions of each of these samples by three density distribution models: exponential distribution, the model of a self-gravitating isothermal disk, and Gaussian density distribution. We found that fits based on models (1) and (3) yield very close results.

The exponential distribution model yields the following vertical disk scale heights: $h_1 = 51 \pm 5$ pc for 69 masers with trigonometric parallaxes, $h_1 = 46 \pm 3$ pc for 59 OB associations, $h_1 = 46.6 \pm 2.8$ pc for 147 H II regions, $h_1 = 64.1 \pm 2.4$ pc for 195 young Cepheids (age ≈75 Myr), and $h_1 = 83.1 \pm 2.4$ pc for 192 old Cepheids (age ≈138 Myr).

An analysis based on the self-gravitating isothermal disk model yields the following vertical disk scale heights: $h_2 = 46 \pm 5$ pc for masers, $h_2 = 36 \pm 3$ pc for OB associations, $h_2 = 35.6 \pm 2.7$ pc for H II regions, $h_2 = 52.1 \pm 1.9$ pc for young Cepheids, and $h_2 = 72.0 \pm 2.3$ pc for old Cepheids.

ACKNOWLEDGMENTS. We are grateful to the referee for helpful remarks that contributed to the improvement of this paper. This study was supported by the “Transient and explosive processes in astrophysics” Program of the Presidium of the Russian Academy of Sciences (P–7).

REFERENCES

Bobylev V. V. 2013, Astron. Lett., 39, 753
Bobylev V. V., Bajkova A. T. 2014, Astron. Lett., 40, 783
Bobylev V. V., Bajkova A. T. 2016a, Astron. Lett., 42, 1
Bobylev V. V., Bajkova A. T. 2016b, Astron. Lett., 42, 182
Bobylev V. V., Bajkova A. T., Shirokova K. S. 2016, Baltic Astronomy, 25, 15
Mel’nik A. M., Dambis A. K. 2009, MNRAS, 400, 518
Mel’nik A. M., Rautiainen P., Berdnikov L. N. et al. 2015, AN, 336, 70
Moisés A. P., Damineli A., Figueredo E. et al. 2011, MNRAS, 411, 705
Rastorguev A. S., Zabolotskikh M. V., Dambis A. K. et al. 2016, arXiv: 1603.09124
Reid M. J., Menten K. M., Brunthaler A. et al. 2014, ApJ, 783, 130
Russeil D. 2003, A&A, 397, 133
Russeil D., Adami C., Georgelin Y. N. 2007, A&A, 470, 161
Wienen M., Wyrowski F., Menten K. M. et al. 2015, A&A, 579, 91